

History of Flux-Density Calibration in Radio Astronomy

Jacob W.M. Baars

Max-Planck-Institute für Radioastronomie
Auf dem Hügel 69,
53121 Bonn, GERMANY
e-mail: jacobbaars@arcor.de.

Abstract

In the course of the last sixty years, radio astronomers have scanned the sky and catalogued millions of cosmic sources, over the entire radio-frequency range from 10 MHz to 1 THz. For the interpretation of the received radiation, it is essential that the observed intensity can be related to an *absolute flux-density scale*, in order to obtain quantities *intrinsic* to the source. The establishment of such a scale has been a painstaking effort over many years, leading to a current accuracy of a few percent over most of the observable frequency range. In this paper, we describe the history of these efforts. We begin with the observations of a few strong sources with small calibrated antennas in the 1960s. We continue up to the recent definitive improvements obtained with large antennas, including interferometer arrays, and spaceborne telescopes operating in the millimeter and sub-millimeter wavelength domains. The review contains an extensive list of references.

1. Introduction: The Need for Absolute Measurements

In the early years of the Jansky-VLA radio telescope in New Mexico, an astronomer on the way to the site drove a part of the 40 km long straight stretch of US Route 60. In the dark, the astronomer might see a car light on the invisible horizon, and wonder how far the distance to the car would be. If the astronomer knew the wattage of its headlight and possessed an eye with calibrated brightness sensitivity, this could be figured out. Alternately, if the astronomer knew the distance, the observed apparent brightness could be turned into the intrinsic brightness of the car's headlight. Even if the distance were unknown, a calibrated measuring device (detector) would provide at least the apparent intensity of the source. Upon arriving at the telescope, the astronomer was faced with a similar problem. In order to turn the output signal of the telescope into a quantity intrinsic to the source, the sensitivity of the

telescope – that is to say, the gain of the antenna and of the receiver system – needed to be known.

In contrast to the astronomer's colleague, the experimental physicist, the observational astronomer is unable to influence the parameters of the physical process the astronomer wants to study. The only measurable data are the properties of electromagnetic radiation emanating from the object of the astronomer's observation. The astronomer can measure the intensity, and possibly the polarization state, as functions of frequency and time. The details are dependent on the sensitivity, along with the frequency and time resolution of the observing device, the telescope and its focal-plane instrument, the last usually called the receiver.

As illustrated in the first paragraph, there exists the difficulty of transferring the measured signal into quantities that are intrinsic to the source. For this, one needs first of all the distance to the object, a notoriously severe problem for sources of continuum radio radiation. Here, the radio astronomer needs the help from his or her "optical" colleague, for instance through the spectroscopic determination of the redshift, and hence distance of the object. There then remains the need to calibrate the received signal in an absolute measure of flux density or brightness temperature. This requires knowledge of the gain of the radio telescope (antenna), and the calibration of the measured antenna temperature at the entrance of the receiver. While the latter can be readily achieved by the so-called "hot-cold-load" comparison method [1], to be discussed below in Section 2.4, the former is practically impossible to determine for a radio telescope of large size reckoned in wavelength.

The lack of knowledge of antenna gain could be circumvented if there were a sufficient number of celestial sources with accurately known absolute intensities over a large frequency range and distributed somewhat evenly across the sky. In fact, this is the usual way in which radio astronomers calibrate the measured flux density of an object, by comparing its signal with that of a known *calibration*

source. The establishment of such a set of calibration sources has been a multi-pronged effort over several decades. It has now reached an accuracy of the order of a few percent over almost the entire frequency range accessible to radio-astronomical observation, roughly from 20 MHz to 1 THz.

It is the purpose of this paper to present the historical development of the subject, by describing the technical efforts needed for achieving its goal, and by summarizing the road towards the current state of affairs in the establishment of an *absolute flux-density scale* at radio wavelengths. Reviews of absolute intensity calibrations in radio astronomy were presented by Findlay [2] and Ivanov and Stankevich [3].

We summarize the process of obtaining the absolute flux density of the strongest radio sources by the use of antennas, the gains of which have been determined by calculation or Earth-bound measurements. These *primary calibrators* are the strongest sources in the constellations Cassiopeia (Cas A), Cygnus (Cyg A), Taurus (Tau A), and Virgo (Vir A). Their strengths can be reliably measured with antennas of an aperture area of the order of 10 m^2 . The gains of such antennas can be calculated in the case of a dipole or horn, or measured on a test range of several hundreds of meters at typical frequencies of the order of 1 GHz. Unfortunately, the strongest sources all exhibit a significant angular size, which requires corrections to the measured signal when observed by large radio telescopes with angular resolutions of the order of the source's angular size or smaller.

The bulk of radio sources is very much weaker than the primary calibrators. Direct comparison between weak and strong objects requires the careful calibration of the gain of the receiver system over a large dynamic range. To avoid this, a set of "secondary calibrators" of intermediate intensity has been created, by accurate relative measurements with respect to the primary calibrators. These are then used as calibrators for the observation of weak objects. The secondary calibrators are normally extragalactic sources of small, or "point-like," angular extent. This avoids size corrections in the flux-density determination, even with observations of high angular resolution, as with interferometers and synthesis telescopes. On the other hand, several of the original secondary calibrators have shown time variability in their luminosity. An important effort has thus been to limit the set of calibration sources to those with stationary flux density. The results of this program were recently published by Perley and Butler [4]. They presented an absolute flux-density scale with an accuracy of a few percent over the frequency range from 1 GHz to 50 GHz. The achievement of this milestone has prompted the writing of this historical review.

It should be noted that the detail of the radio *spectrum*, i.e., the flux density as a function of frequency, is one of the essential—and often, the only—data in the study of continuum radio sources such as quasars, supernova remnants, and HII-regions. It is thus important that a reliable flux-density scale over an extended frequency range be established.

It has been customary, based on theoretical grounds and supported by observations, to express the spectrum of a source by a power-law function. The *spectral flux density*, S , as a function of frequency, ν , can thus be written as $\log S = a + b \log \nu + c \log^2 \nu + \dots$. Plotted on a log-log scale, many sources exhibit a straight line ($c = 0$). The parameter b is called the *spectral index*, often denoted by α . These parameters provide information on the physical mechanism responsible for the radiation. Curved spectra with $c \neq 0$ are more informative, but a reliable measurement of c requires an accurate calibration.

By the time of the publication of large catalogues of radio sources in the early 1960s, spectral flux density was normally expressed in *flux units*, with $1 \text{ fu} = 10^{-26} \text{ Wm}^{-2} \text{ Hz}^{-1}$. Although not fitting in the SI system of units, this was adopted in 1973 by the International Astronomical Union as the *unit of flux density*, and given the name *Jansky* ($1 \text{ Jy} = 10^{-26} \text{ Wm}^{-2} \text{ Hz}^{-1}$). Its use has been widely adopted across the electromagnetic spectrum, well beyond radio astronomy.

2. Determination of Antenna Gain

Radio astronomy was born in 1932 by Karl G. Jansky's discovery of Galactic radiation at a frequency of about 20 MHz [5]. A follow-up was made by Grote Reber, who built a 9.6 m-diameter paraboloidal dish in his backyard, and successfully mapped part of the sky at the frequency of 160 MHz [6]. After World War II, groups of radio and radar engineers started to use their equipment to look at the "sky," notably in England, Australia, and the USA. The frequency range used was from several tens to a few hundreds of MHz, covered with dipole-array antennas, which were often used in an interferometer configuration to improve the angular resolution. Where dish antennas were available, notably in Europe and the USA, the frequency range was extended to higher frequencies. These eventually reached several gigahertz around 1950, and lead to the detection of the spectral line of neutral atomic hydrogen at 1420 MHz in 1951 by Ewen and Purcell [7a] and Muller and Oort [7b].

It must be considered a lucky circumstance that the strongest cosmic radio sources, Cas A and Tau A, being supernova remnants, and Cyg A, a radio galaxy, emit predominantly synchrotron radiation, which exhibits a spectrum at radio wavelengths with increasing intensity towards lower frequencies. This enabled researchers to detect them in the early stages of their instrumental developments. Eventually, observational radio astronomy reached a point where accurate knowledge of the spectrum was needed to study the details of the physical process by which the sources radiate. This involved consideration of the absolute calibration of the observed flux density, and the need to have antennas with a well-known gain.

Two types of antennas allow a theoretical calculation of the gain from physical dimensions: the dipole and the

pyramidal horn. Their characteristics are summarized in the following sections.

2.1 The Dipole and Dipole Array

The derivation of the radiation characteristics of a dipole can be found in any textbook on electromagnetic theory, e.g., [8]. As an illustration, we mention here the results for an elementary electric dipole and a wire antenna, fed in the middle and a half-wavelength long, the so-called half-wave dipole. The radiation power patterns of these are represented by

$$P_{el} \propto \sin^2 \theta \quad \text{elementary dipole} \quad (1)$$

$$P_{hw} \propto \left[\frac{\cos(\pi \cos \theta / 2)}{\sin \theta} \right]^2 \quad \text{half-wave dipole} \quad (2)$$

The pattern is uniform in the plane perpendicular to the dipole, and has its maximum in the equatorial plane. The meridional patterns of the expressions above are shown in Figure 1. Integrating over the patterns, the gains are found to be:

$$G_{el} = 1.50 \quad (1.76 \text{ dB}) \quad \text{elementary dipole},$$

$$G_{hw} = 1.65 \quad (2.17 \text{ dB}) \quad \text{half-wave dipole}.$$

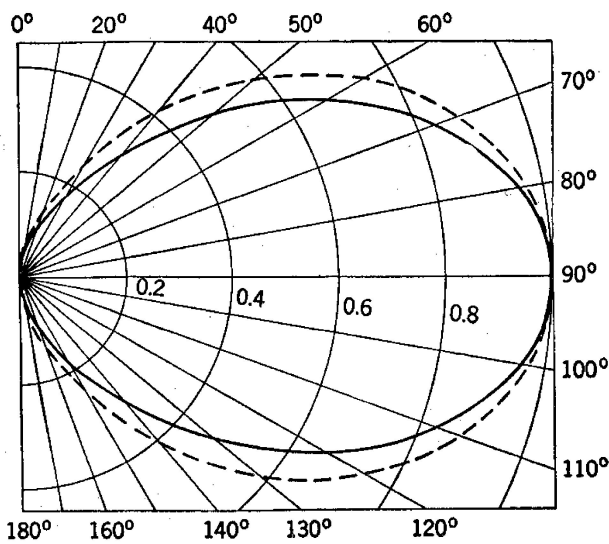


Figure 1. The meridional polar power diagram of the half-wave dipole (full line) and the elementary dipole (dashed). The half-power beamwidth of the half-wave dipole is about 80°.

The fortuitous increase of flux density of the strongest sources towards low frequencies made it possible to use dipoles, suspended over a reflecting ground plane, as an antenna. In most cases, a pair of half-wave dipoles was used as an interferometer, or an array of half-wave dipoles was used, which provided a higher antenna gain.

It is of some interest to mention here the possibility of obtaining absolute calibration by the use of an interferometer consisting of a large, sufficiently sensitive, but uncalibrated element, and a small, absolutely calibrated second element. This was pointed out and applied by Seeger [9], who obtained an absolute flux density of Cas A at 400 MHz with an interferometer consisting of a horn with a calculated gain and a 7.5 m diameter "Würzburg" reflector antenna. The interferometer was needed because the gain of the small horn was insufficient to make a direct absolute total-power measurement. Later, big horns were constructed specifically for such absolute measurements, as shall be described below.

With this method, the observation of the source involves two steps:

1. Interferometric measurement with the small, calibrated antenna and the large antenna;
2. Total power measurement with the larger, sufficiently sensitive, but uncalibrated reflector.

We obtain the following output signals, expressed in power, P . The total power measurement of the large antenna is

$$P_t = S g_t A_t ,$$

and the output of the interferometer of the horn and large antenna is

$$P_h = S (g_t A_t g_h A_h)^{0.5} ,$$

where S is the unknown flux density of the source, g_t and g_h are the electronic gains of the two receivers on the antennas, and A_t and A_h are the effective areas of the large antenna and the horn, respectively. The electronic gain can be accurately measured (to be discussed below). Accounting for those, we can write the following expression:

$$A_t = \left(\frac{P_t}{P_h} \right)^2 \frac{g_h}{g_t} A_h . \quad (3)$$

Alternatively, one can eliminate A_t and obtain the flux density, S .

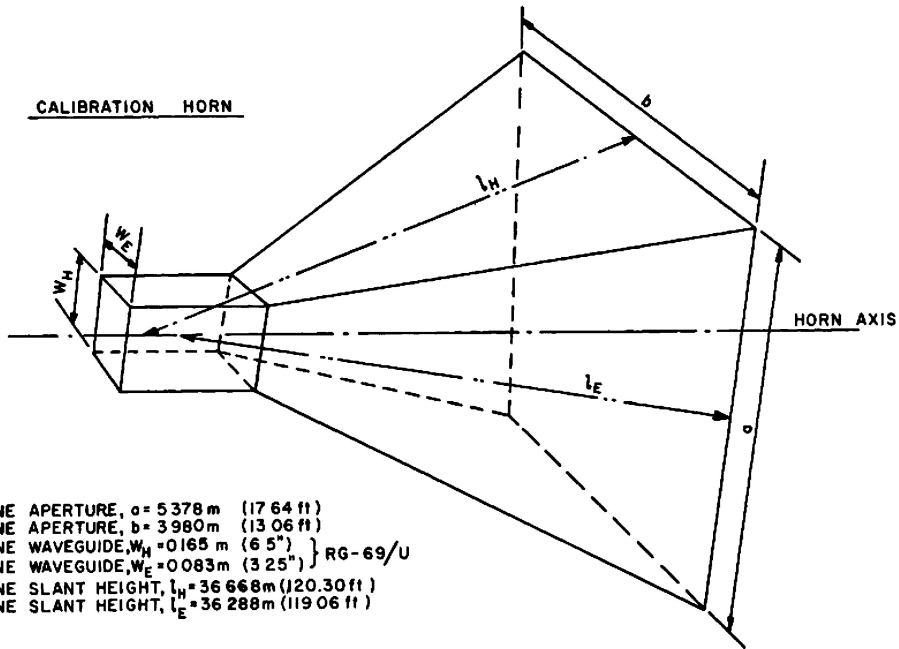


Figure 2. Illustrating the geometry of the pyramidal horn. The numerical data in the drawing pertain to the Little Big Horn at NRAO (see text; after Findlay et al. [16]).

Wyllie [10] used the large Molonglo Cross antenna in Australia by forming interferometers between the two sections of the E-W arm of the cross, and a reference antenna consisting of an array of 16 half-wave dipoles, separated by 0.75 wavelength, placed 0.25 wavelength above a reflecting ground screen. The gain of this dipole array was computed, based on theory by Schelkunoff and Friis [11], and measured to be 76.2 (18.82 dB), to an accuracy of better than 3%. The measurement of the beam pattern confirmed the calculated gain. In this case, the actual observations were done with

1. Three interferometer pairs (a reference antenna with each of the east and west arms of the cross, and between the two arms); and
2. An interferometer between the reference antenna and the whole E-W arm, plus a total power measurement with the full arm.

From these data, the unknown gain of the large cross arms was eliminated, leading to an absolute measurement of the flux density of the relatively weak source. We return to this later.

2.2 The Pyramidal Horn Antenna

Schelkunoff presented the gain of an electromagnetic pyramidal horn in his well-known book, *Electromagnetic Waves* [12]. If we denote the aperture width in the H plane by a , in the E plane by b , and corresponding slant lengths by l_a and l_b , we have the following equations for the gain (Figure 2). For the E-plane sectoral horn,

$$G_E = \frac{64al_b}{\pi\lambda b} \left[C^2 \left(\frac{b}{\sqrt{2\lambda l_b}} \right) + S^2 \left(\frac{b}{\sqrt{2\lambda l_b}} \right) \right], \quad (4)$$

and for the H-plane sectoral horn,

$$G_H = \frac{4\pi bl_a}{\lambda a} \left\{ [C(u) - C(v)]^2 + [S(u) - S(v)]^2 \right\}, \quad (5)$$

where

$$u = \frac{1}{\sqrt{2}} \left(\frac{\sqrt{\lambda l_a}}{a} + \frac{a}{\sqrt{\lambda l_a}} \right),$$

and

$$v = \frac{1}{\sqrt{2}} \left(\frac{\sqrt{\lambda l_a}}{a} - \frac{a}{\sqrt{\lambda l_a}} \right),$$

and $C(x)$ and $S(x)$ are the well-known Fresnel integrals. The gain of the pyramidal horn takes the form

$$G = \frac{\pi}{32} \left(\frac{\lambda}{b} G_H \right) \left(\frac{\lambda}{a} G_E \right). \quad (6)$$

These gain expressions have been checked by careful laboratory measurements, and have shown general agreement to about 1%. In some cases, such measurements were extended to rather large horn antennas, as in the work of Jull and Deloli [13] on the horn-paraboloid with an aperture of 8 m^2 at the Algonquin Radio Observatory in Canada.

2.3 The “Artificial Moon” Method

A major problem in the accurate measurement of the gain of a large aperture antenna is the finite distance to a terrestrial signal source. When the source is closer to the antenna under test than the so-called far-field distance, the incoming phase front is not closely an equiphasic surface. A number of corrections then need to be made, which are strongly dependent on the distance between the source and the antenna. The far-field distance is defined as

$$R_f = 2D^2/\lambda, \quad (7)$$

where D is the diameter of the antenna and λ is the wavelength. For $D = 10 \text{ m}$ and $\lambda = 10 \text{ cm}$, this distance is already 2 km. Rarely will there be a possibility to place the source at a decent elevation angle, of the order of 10° , so that ground effects can be ignored.

Nevertheless, in the early 1960s, Troitskii and Tseitlin [14], at the Radiophysical Research Institute in Gorkii (now Nizhny Novgorod), Russia, introduced a method of calibrating relatively small antennas by moving a black disc in and out of the antenna’s beam at a certain distance from the antenna (Figure 3). They coined the name *artificial moon* method for this procedure. In their first experiments, they chose a distance equal to the far-field distance, and a size of the black screen that subtended an angle significantly smaller than the primary beamwidth of the antenna. Later, the method was developed to allow measurements in the near-field region of the antenna by introducing correction factors. It has been applied over a large frequency range, from roughly 300 MHz to 10 GHz. Several antenna sizes were used to obtain sufficient signal-to-noise ratio (SNR) for the accurate measurement of the antenna temperature of the strongest sources, such as Cas A, Cyg A, and Tau A.

This method differs from the usual antenna test range in that it uses an extended “blackbody” source as transmitter, instead of a monochromatic, point-like signal source. The “broadband” radiation from the black disc is accepted over the full bandwidth of the receiver system, which will later be used to measure the intensity of a cosmic source. The choice of using a source of finite angular extent means that it “fills” part of the primary beam-lobe of the antenna. If the disc subtends a solid angle of Ω_d as seen from the antenna, and is smaller than the antenna’s main-beam solid angle, Ω_m , we can define the *effective* disc solid angle as

$$\Omega'_d = \int_{\Omega_d} f(\theta, \phi) d\Omega, \quad (8)$$

where $f(\theta, \phi)$ is the antenna’s beam. The measured antenna temperature difference between the situation with the disc and with the disc removed can be written as

$$\Delta T_A = (T_D - T_B) \Omega'_d, \quad (9)$$

where T_D and T_B are the temperatures of the disc and the sky background behind the disc, respectively.

If the black disc just fills the full main beam to its first null, the measured antenna temperature difference is $\Delta T_A = \eta_B (T_D - T_B)$, where η_B is the *beam efficiency* of the antenna. In this case, one thus measures the antenna’s beam efficiency, η_B , instead of the aperture efficiency, η_A as in the case of a point source. The aperture efficiency can be calculated from the measured beam efficiency from the equation

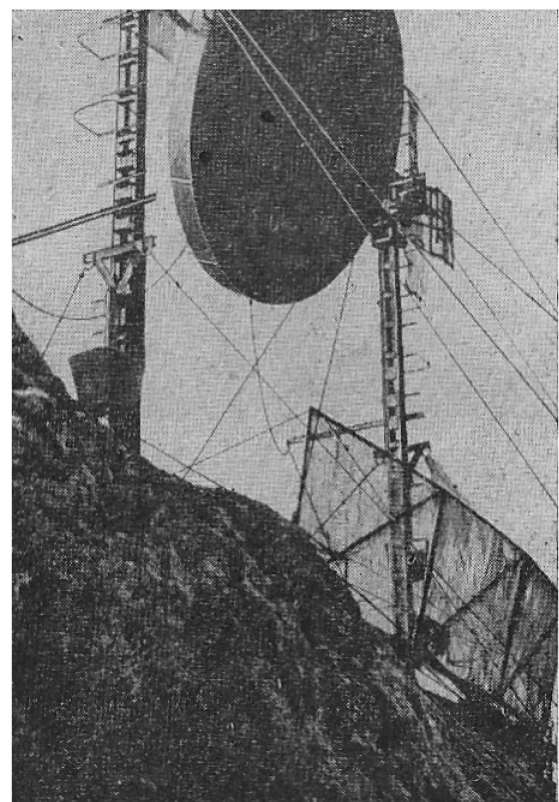


Figure 3. The “artificial moon,” a round “black disc” suspended between towers on a promontory at some distance from the antenna under test. The cable network allowed the disc to be moved in and out of the beam, without significantly changing the influence of the installation on background radiation.

$$\eta_A = \frac{\lambda^2}{\Omega_m A_g} \eta_B, \quad (10)$$

where Ω_m is the main-beam solid angle, and A_g is the geometrical area of the reflector's aperture.

Note that one also needs to determine the main beam's solid angle. This requires knowledge, either by calculation or measurement, of the main beam to the level of the first null in its pattern. This is not a trivial matter, in practice. For details on this aspect, see, for instance, Baars [15, Section 5.3.3].

2.4 Receiver Calibration

As was mentioned earlier, the recorded signal at the output of the receiver system needs to be expressed in an equivalent increase of the *antenna temperature*, T_A , measured at the input port of the receiver. For a point source, the relationship between source flux density, S_ν , and the antenna temperature is given by the relation

$$S_\nu A = 2kT_A, \quad (11)$$

where A is the absorption area of the antenna, and $k = 1.38 \times 10^{-23} \text{ WK}^{-1}\text{Hz}^{-1}$ is Boltzmann's constant. The calibration of T_A is normally achieved by the so-called *hot-cold-load* method. By connecting the input of the receiver alternately to matched resistive loads at different

and well-known physical temperatures, the sensitivity scale of the receiver can be expressed in terms of the equivalent temperature of the input signal (Figure 4).

To avoid errors due to possible nonlinearity of the amplifier chain in the receiver, one chooses the temperature difference between the two loads to be of the same order as the expected antenna temperature from the source. While in principle simple, this measurement needs careful consideration of proper matching between the receiver and the changing inputs from loads and antenna, as well as any losses in the intermediate connections. The trace of a single observation of Cas A with the Little Big Horn (LBH) at NRAO Green Bank [16] illustrates the procedure (Figure 5).

3. Review of Absolute Measurements

3.1 Summary of Methods of Measurements

Many absolutely calibrated observations of the strongest sources were obtained in the period 1960-1970. Source catalogues were becoming available over a growing range of frequencies. The establishment of reliable radio spectra over a substantial frequency region was essential for the astrophysical interpretation of the observations. We now summarize the absolute measurements of flux density that were obtained, separated by the different methods and equipment.

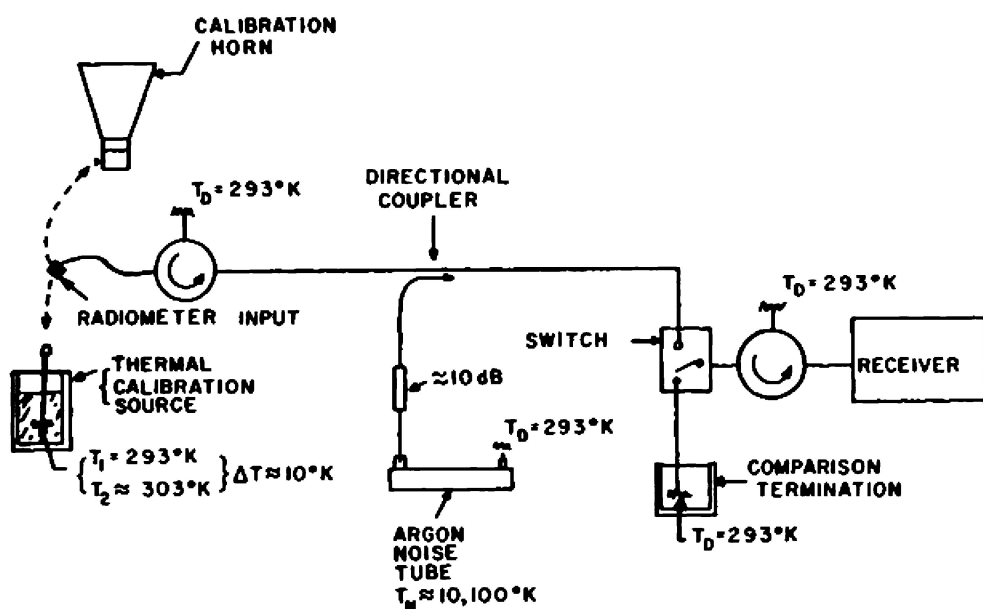


Figure 4. The receiver layout with calibration devices (noise tube and thermal calibration source) of the Little Big Horn experiment at NRAO, Green Bank (after Findlay et al. [16]).

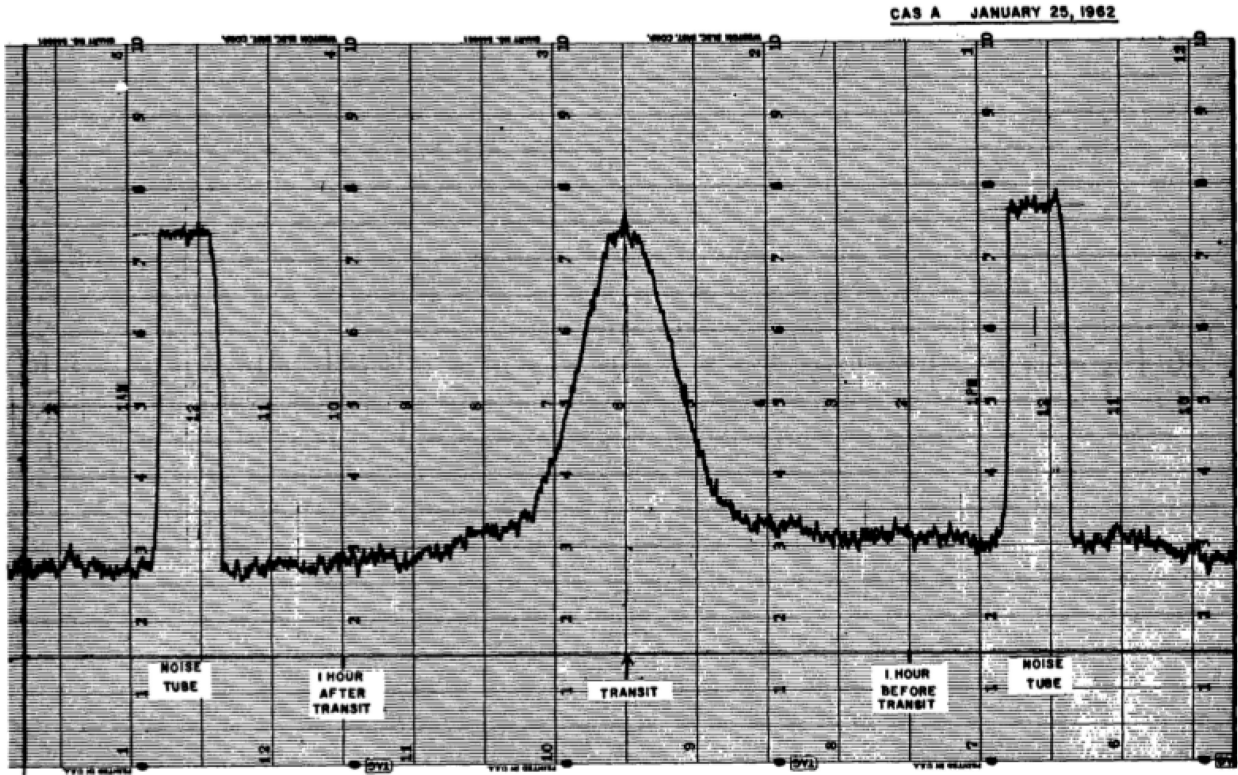


Figure 5. An example of the drift scan of Cas A through the beam of the Little Big Horn, with calibration marks from the noise source on both sides (after Findlay et al. [16]).

3.1.1 Low Frequency: Dipoles

Parker [17] carried out a carefully conducted experiment in 1966 in Cambridge, UK, at frequencies of 38.0 MHz, 81.5 MHz, and 152.0 MHz, with a simple interferometer consisting of two single dipoles. The theoretical calculations of gain and antenna pattern were compared to pattern measurements using Cas A and Cyg A, leading to the conclusion that the gain was accurate to 2.5%. Other accurate dipole measurements were reported by Roger et al. [18] at 22 MHz, and Viner [19] at 26 MHz. The quoted accuracies were in the 4% to 5% range. Somewhat less accurate (10% to 14%) results were given for the work by Bridle [20] at 10 MHz and Braude et al. [21] at five frequencies between 12 MHz and 25 MHz. In the latter program, the large array in the Ukraine was used in a similar manner as by Wyllie, described above. Wyllie [10] used the Molonglo Cross antenna in Australia at 408 MHz for absolute measurements of the flux density of a number of relatively weak sources (30 Jy to 70 Jy) with a reported accuracy of 5%.

3.1.2 Mid to High Frequencies: Horns and Horn-Paraboloids

Observations of the strongest sources from about 300 MHz up to 16 GHz were made with horn antennas. The

first was by Charles Seeger [9], who used an interferometer of a horn and a 7.5 m reflector to measure the absolute flux density of Cassiopeia A at 400 MHz at the Dwingeloo Observatory in 1955. In a footnote to his short paper, he “strongly recommended that horns be used as antenna gain standards in radio astronomy whenever it is desired to measure absolute flux densities to an accuracy of better than 1 dB.” His own single measurement of Cas A yielded a flux density of 5620 Jy (epoch 1955.6), with an estimated maximum error of 15%. Actually, he should have obtained about 7000 Jy, which is 25% above his measurement, and perhaps illustrates the difficulty of making absolutely calibrated observations. At the IAU Symposium No. 5, “Radio Astronomy,” in 1955, Seeger [22] emphasized the importance “to establish the spectra of a few *reference sources*.” He presented the situation with the Cas A spectrum, which was based on some 15 observations with quoted accuracies of 10% to 30%. He noted, “Absolute flux density measurement appears to be simple...but has turned out to be unexpectedly difficult.”

In any case, the superiority of the horn antenna for accurate absolute calibration was recognized, and by the mid-1960s, several horns were in use for this purpose.

Around 1960, in Canada, Broten and Medd [23] and McCrae and Seaquist [24] used horn antennas at 3200 MHz and 320 MHz, respectively, quoting an error of 5%. At the National Radio Astronomy Observatory (NRAO) in Green



Figure 6. The Little Big Horn at the NRAO, Green Bank. The aperture was $5.4 \text{ m} \times 4.0 \text{ m}$, and the length was about 36 m. Cas A crosses the beam daily, and a measurement of its flux density is made at 1440 MHz (NRAO/AUI/NSF).

Bank, Findlay built the Little Big Horn (Figure 6). This was a fixed antenna, used to daily measure the flux density of Cassiopeia A to an accuracy of 2% to 3% at a frequency of 1440 MHz for a period of several years in the early 1960s, and again in 1969-1971 [16, 25].

Medd [26] used a horn-paraboloid at the Algonquin Radio Observatory in Canada at frequencies of 3200 MHz, 6660 MHz, and 13490 MHz. This horn was carefully analyzed and measured by Jull and Deloli [13], who

obtained agreement between theoretical calculation and measurement of the gain to about 1% accuracy. Allen [27] observed with the horn at Lincoln Laboratories at 8250 MHz and 15500 MHz. Finally, the horn-paraboloid at the Bell Labs in Holmdel, NJ, delivered data at 1415 MHz [28], 4080 MHz [29, 30], and 16000 MHz [31, 32]. This is the same horn with which Penzias and Wilson separated the cosmic microwave background of 2.7 K from the other sources of noise in their system (Figure 7). The errors quoted for these observations, which were carried out between 1962 and 1970, ranged between 2% and 5%.

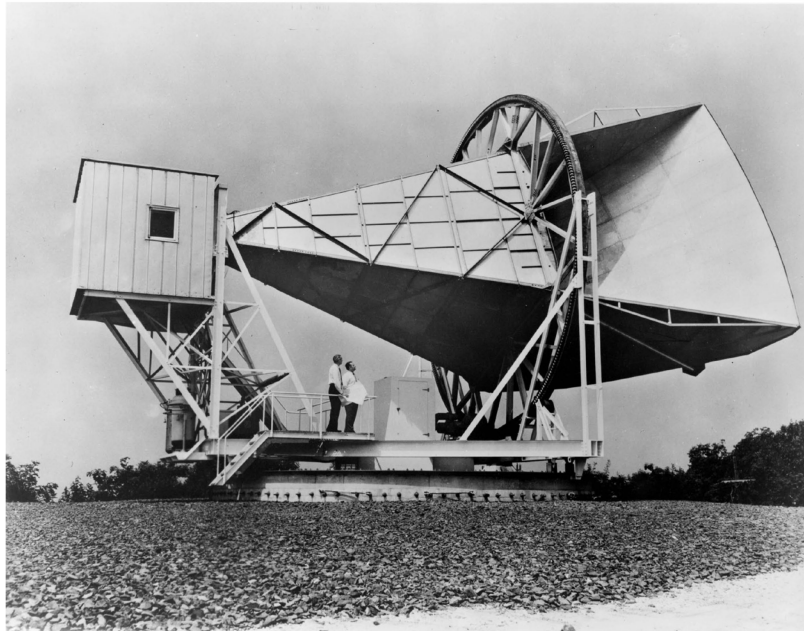


Figure 7. The large horn-paraboloid at the Bell Telephone Laboratories in Holmdel, New Jersey. The aperture was $6 \text{ m} \times 6 \text{ m}$, and its length was about 15 m. Absolute flux densities of Cas A were obtained at 1415 MHz, 4080 MHz, and 16000 MHz. The cosmic microwave background was detected with this instrument by Penzias and Wilson in 1965. The antenna at its original site was designated a National Historic Landmark in 1988 (AT&T).

3.1.3 Mid Frequencies: Artificial Moon

The *artificial moon* (AM) method has been described in Section 2.3. It should be noted that refinements in the experimental method led researchers to apply corrections to earlier measurements made before 1963. However, all data published up to the mid-1970s had quoted errors in the 3% to 6% range. Many measurement series of Cas A were reported over the frequency range from 550 MHz to 9380 MHz by Bondar et al. [33], Dmitrenko et al. [34], and Vinogradova et al. [35]. Ivanov and Stankevich [3] presented an extensive survey of the subject, entitled “Absolute Flux Scale for Radio Astronomy,” in the Russian journal *Radiofizika* (1986). Despite the publication of a translation in English (*Journal Radiophysics and Quantum Electronics*), the article appears to have drawn little attention among Western radio astronomers. An important feature of the Cas A measurements with the artificial moon method is the slightly but consistently steeper spectrum than that obtained by using “Western” measurements with horns.

Ivanov and Stankevich argued that the horn measurements showed inconsistencies within the measurements by each of three different author groups [26-32]. The current author found no inconsistency in any of the three groups of data. The published gain values at the different measurement wavelengths follow quite precisely the expected wavelength-squared relation. There are good arguments to trust the calculations of horn gain, and moreover, several of the horn gains were also experimentally determined. On the other hand, all artificial moon measurements were carried out with essentially similar equipment and identical procedures to correct for systematic errors, such as background subtraction, “blackness” of the disc, Fresnel-field correction, atmosphere, etc. Any error in these corrections would propagate through all measurements, and could introduce an undetected systematic effect.

3.2 Secular Decrease of Cassiopeia A and Taurus A

3.2.1 Cassiopeia A

Cassiopeia A is a rather recent supernova remnant (CE 1680). Shklovskii [36] calculated an expected secular decrease in its flux density of approximately 2% per annum, which in his simple source model was independent of frequency. Based on data collected over 12 years at a frequency of 81.5 MHz, Högbom and Shakeshaft [37] determined a rate of decrease of $1.06\% \pm 0.14\%$ per year. Data at higher frequencies became available, and by the mid-1960s, a generally accepted value of the secular decrease was $1.1\% \pm 0.15\%$ per year. In the early 1970s, evidence was growing that the secular decrease was frequency dependent. Based on accurate relative measurements, Baars and Hartsuijker [38] obtained a value of $0.90\% \pm 0.12\%$ at 1.4 GHz and 3 GHz, significantly smaller than the updated value from Scott et al. [39] of $1.29\% \pm 0.08\%$ at 81.5 MHz. Further data obtained by Dent et al. [40], Read [41], and Stankevich et al. [42] confirmed the frequency dependence of the secular decrease. Based on these data, Baars et al. [43] derived the following relationship for the secular decrease of the flux density of Cassiopeia A as a function of frequency:

$$d(\nu) = 0.97(\pm 0.04) - 0.30(\pm 0.04) \log \nu, \quad (12)$$

with d in percent per year and ν in GHz.

The group around Stankevich at Gorkii has made an exhaustive study of the evolution of the Cas A spectrum, mainly based on observations with the *artificial moon* system. Stankevich et al. [44] summarized their work in

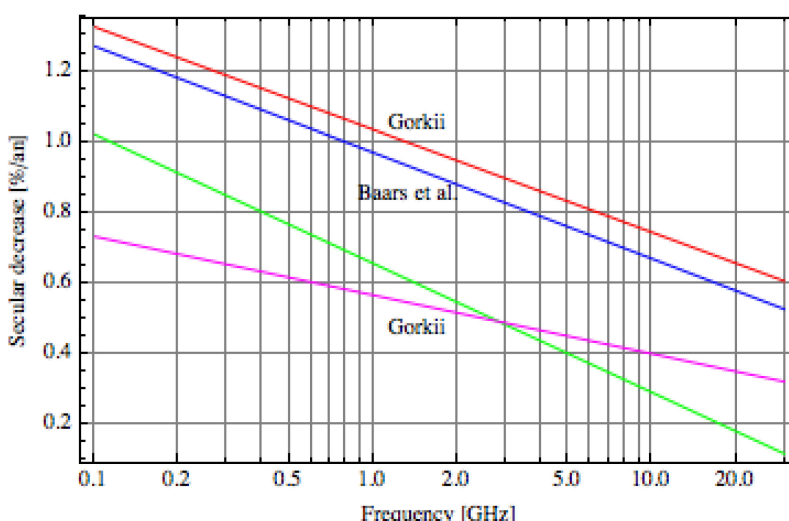


Figure 8. The secular decrease in the flux density of Cas A in percent per year as a function of frequency. The red and blue lines refer to measurements at Gorkii and the derivation by Baars et al. over the period 1960-1975. The green line applies to 1969-1984. The magenta line is for the period after 1984 to 2000 from the Gorkii data.

1999, and arrived at a secular decrease in the range from 0.5 GHz to 10 GHz for the period 1961-1975 given by

$$d(\nu) = 1.035 - 0.29 \log \nu \quad (13)$$

with d in percent per year and ν in GHz. Both results are shown in the graph of Figure 8. They appear to be offset from each other by about one sigma, while the slopes are nearly equal. Note that the data sets are quite different. Only two Gorkii data points were used in the blue Baars et al. result, while only Gorkii data were included in the red line.

From their extended study of Cas A, the group at Gorkii concluded that the secular decrease is not uniform over time, and also appears to vary over frequency [44]. The green line in Figure 8 shows their analysis for the period 1969-1984. The flux decrease has slowed down at all frequencies, and apparently somewhat faster at high frequencies. The fit to the data for the period after 1984, presumably up to the late 1990s, is shown as the magenta line, indicating an accelerated decay at centimeter wavelengths and a slower decay at decimeter wavelengths. This suggests a strong overall drop in the secular decrease rate after 1969 and a change in frequency dependence after 1984. Observations near 15 GHz by O'Sullivan et al. [45] supported some of this trend, as did the value of $0.394\% \pm 0.014\%$ per year at 30 GHz, determined from 2001-2004 by Hafez et al. [46].

The time- and frequency-dependent behavior of the luminosity of Cas A complicates the use of its radio spectrum as a basis for the establishment of an absolute flux-density scale. In Section 4, we discuss the absolute spectrum of Cas A, which is based on many measurements in the frequency range from roughly 100 MHz to 30 GHz. It is fortuitous that all those data were collected in the period between 1960 and 1973, the large majority between 1965 and 1970. The good agreement in the secular decrease over that relatively short period between the Gorkii group and Baars et al. supports the reliability of the Cas A absolute spectrum. Because the main purpose of the present paper is to illustrate the historical development of the *absolute flux-density scale*, we shall not discuss the interesting aspects of the evolution of Cas A, as shown in the observations after 1970, any further.

3.2.2 Taurus A

Taurus A is the remnant of the supernova of CE 1054, and it is a well-studied source at radio wavelengths. Because of its intensity, it has also been observed with small, absolutely calibrated antennas. A small secular decrease has been measured of $0.17\% \pm 0.02\%$ per year at 150 MHz and 950 MHz [47], $0.167\% \pm 0.015\%$ per year at 8 GHz [48], and $0.22\% \pm 0.07\%$ per year at 33 GHz [46]. This suggests a time- and frequency-independent secular decrease of about 0.2% per year over the period 1970-2004.

4. Towards an Absolute Flux-Density Scale

4.1 Development Over Time, Improvement of Accuracy

4.1.1 Reliable Source Spectra

In one of the first papers on “the spectra of radio stars,” Whitfield [49] pointed to the need to construct the spectra (the dependence of flux density on frequency) of the new radio sources to help understand their characteristics and to separate different classes of sources by the difference in spectral index. He suggested the use of Cas A, being the strongest source, as a standard against which the relative intensities of other sources could be determined by measuring the ratio. To transfer those to absolute flux densities, the Cas A spectrum would need to be absolutely known. He used five available absolute measurements between 38 MHz and 400 MHz to derive a power-law spectrum for Cas A with a spectral index of -0.8 . It is interesting to note that the flux-density scale most widely used over the last 35 years and discussed in detail below is based on a value of -0.792 .

Around 1960, extensive catalogues of radio sources became available through the surveys conducted notably at Cambridge, Jodrell Bank, Caltech, and CSIRO. Most of these were done at frequencies between 80 MHz and 1400 MHz. Essentially all authors referred to the difficulty of putting the observed intensities on an absolute flux-density scale. Seeger [9] had already mentioned this problem.

In an important step towards establishing reliable spectra of a large number of radio sources, Conway, Kellermann, and Long (CKL) [50] considered observations in the frequency range of 38 MHz to 3200 MHz. An absolute flux-density scale was obtained by a somewhat convoluted procedure, whereby an available absolute measurement of Cas A at a particular observing frequency (38 MHz, 400 MHz, 1420 MHz, and 3200 MHz) was used as the basis. They picked seven sources of moderate strength, fitted a power law through the flux densities at 38 MHz, 410 MHz, and 1420 MHz, and consecutively defined the flux-density scale at the intermediate frequencies (178 MHz, 240 MHz, 710 MHz, and 958 MHz), so that the mean flux density of the seven sources at each frequency fitted the power law.

Kellermann [51] observed about 200 sources, mainly from the 3C and Sydney catalogues, at frequencies of 475 MHz, 710 MHz, 958 MHz, 1420 MHz, and 2841 MHz with the Caltech interferometer. For the flux-density calibration, he established an absolute spectrum of Cas A, applying a 1% per year secular decrease of its flux density at all frequencies. From this Cas A spectrum, contrary to the individual absolute measurements used by CKL, he

then established *preliminary* (his emphasis) calibrations of Cyg A, Tau A, and Vir A at all frequencies where accurate ratios with respect to Cas A were available. As a final step he used existing, accurate ratios of five moderately strong sources (3C123, 3C348, 3C353, 3C380, 3C409) with respect to the four *primary calibrators* to determine their power-law spectra. The *secondary* calibrators formed the basis for the calibration of all other sources up to 1420 MHz. Kellermann's method minimized the effects of systematic errors in the individual absolute calibrations of Cas A.

Kellermann, Pauliny-Toth, and Williams (KPW) [52] presented the spectra of the entire revised 3C catalogue between 38 MHz and 5000 MHz in 1969. The flux-density scale was based on the Cas A spectrum, which was derived from 15 accurate absolute determinations available at the time. Also there, a set of four secondary standards with straight spectra (3C218-Hya A, 3C274-Vir A, 3C348-Her A, and 3C353) was selected.

4.1.2 Absolute Antenna Gain Calibration

In the same period – the late 1950s and early 1960s – there was great activity in the construction of large and more-precise reflector antennas for radio astronomy. This was soon followed by large paraboloids used as ground stations in satellite communication and deep-space tracking. From the engineering side, the interest grew to fully characterize the new antennas and to study their behavior in operation. It was a natural step for radio astronomers to use the strongest radio sources as broadband signal radiators for their antenna measurements. Soon, managers and engineers of communication and deep-space tracking ground stations used the strong radio sources as test transmitters and the radio astronomical methods for the characterization of the antennas. These methods are discussed in detail in [15].

The stronger the test source, the more accurate would it be possible to characterize the antenna parameters. In the early days, the sun was often used for this purpose. However, the sun is far from an ideal calibrator. At long wavelengths, its intensity is extremely variable, and its angular diameter of about a half degree is much larger than the beamwidth of the large antennas operating at short, cm wavelengths. It was thus natural to concentrate on the strongest sources, Cas A, Cyg A, and Tau A. These were the sources of (forced) choice when, during the 1963–64 winter, Peter Mezger, with his assistants Heinz Wendker and the author, undertook to characterize the NRAO 300-ft and 85-ft telescopes in Green Bank at the short (beyond design specification) wavelengths of 10 cm and 2 cm, respectively. The antenna beamwidths in these cases are about 4 to 5 arcminutes, comparable to the angular sizes of Cas A and Tau A.

To obtain as accurate a measurement of antenna gain as possible, it was decided to make a comprehensive study of the available absolute measurements of these

sources, carefully applying all necessary corrections for polarization and angular size. Once this was done, up to the highest measurement frequency of 15 GHz, significantly improved absolute spectra of the three strongest sources were obtained by inclusion of several recently published accurate absolute measurements, and locally performed additional relative measurements among the strong sources, at frequencies above 3 GHz. The submission of this work for publication met with strong objection from the referee of the *Astrophysical Journal* on the argument that the paper did not contain any new astrophysical insight. In the end the *Astrophysical Journal*'s Editor accepted the authors' argument that the time had arrived to treat observational radio astronomy as a quantitative experimental science (Baars, Mezger, Wendker (BMW), [53]).

The characterization of the antennas provided useful input to the understanding of their behavior, and some hints as to the feasibility of the homologous structural design method, which was being developed at NRAO by von Hoerner [54] at the same time. For instance, the loss of gain at small elevation angles of the reflector could be partially recovered by an adjustment of the position of the feed along the axis of the antenna (axial focusing). This meant that the antenna deformed to approximately a paraboloid, albeit with a different focal length.

As an example from outside astronomy, in the mid-1970s, the European Space Agency (ESA) launched the Orbiting Test Satellite (OTS). It was desired to measure on Earth the absolute power transmitted by its beacon at 12 GHz, in order to check any influence of the launch and deployment on the OTS system. It was also desired to provide a source of known intensity from the OTS for other ground stations in the new satellite band at 12 GHz. For this to be successful, ESA needed at least one ground station to be fully calibrated. The author was asked to help in achieving this with the aid of the strong radio sources. In the spring of 1977, the gain of the 12-m diameter antenna at the Fucino station in Italy was determined with an absolute accuracy of better than 5%.

4.2 Extension of Frequency Range

In the latter part of the 1960s, several accurate horn measurements of Cas A were made up to frequencies of 20 GHz. Absolutely calibrated measurements with dipoles were made at low frequencies of 38 MHz, 81.5 MHz, and 152 MHz. A large amount of data between 0.5 GHz and 9.4 GHz also became available from the group at Gorkii, using their *artificial moon* method.

When Ard Hartsuijker and the author compared their measurements of the ratios of the flux density between the strongest sources, obtained with the Dwingeloo telescope at 21 cm and 11 cm wavelengths in the period 1968 to 1971, with those of several observers at epoch 1956–1961 made with telescopes of the same size (and hence, equal

beamwidth), they obtained a value of $0.9\% \pm 0.1\%$ per year for the decrease in flux density at both frequencies. This value was significantly smaller than the recently updated value of 1.29% per year at 81.5 MHz [39]. Realizing that a frequency-dependent secular decrease would influence the spectrum as derived by BMW, and thereby source flux-density scales, they undertook a new analysis of the Cas A absolute spectrum, including all new data up to 1971 (Baars and Hartsuijker (BH) [38]).

Taking values for the secular decrease of 1.3% , 1.1% , and 0.9% in the frequency ranges < 300 MHz, 300 MHz to 1200 MHz, and > 1022 MHz, respectively, they reduced all data to epoch 1965, which was the approximate midpoint of all measurements used in the analysis. The resulting spectrum of Cas A could be fitted closely with a single power law with spectral index $-0.787\% \pm 0.006\%$ up to 16 GHz, if one took into account that the 38 MHz point was already influenced by the downward tendency of the spectrum indicated by observations at even lower frequencies.

Apart from suggesting frequency dependence in the decrease of the Cas A flux density, these authors also commented on the corrections to be made to the existing flux-density scales from CKL, Kellermann, and KPW. These were significant at frequencies below 1 GHz. For instance, the CKL scale at 400 MHz needed an upward correction of 9.2% . This was confirmed by Conway and Munro [55], who compared the CKL scale with the scale by Wyllie [10], which was based on absolute measurements of five sources of medium intensity (~ 40 Jy). They concluded that CKL was $8.7\% \pm 1.6\%$ low. Although these authors mentioned the BH paper in their article, they apparently overlooked the conclusion in that paper about the necessary correction factors. It is of some interest to note here that the CKL scale near 400 MHz was strongly influenced by the absolute measurement of Seeger [9], which, as we have noted above, was more than 20% low. If the early data point from Seeger had been more correct, the adjustment of the CKL scale some six years later would perhaps not have been necessary.

The KPW scale did require smaller corrections on the basis of the BH scale, less than 3% above 1 GHz, increasing to about 8% at 178 MHz.

The importance of the work by Wyllie [10] should be emphasized here, because he established an independent scale at 408 MHz that does not depend on Cas A. His method was described in Section 2.1. On his scale, the flux density of Cas A was 6555 Jy (epoch 1965.0) at 408 MHz, while the BH spectrum yielded 6450 ± 75 Jy, 1.5% below Wyllie's value. (On the final BGPW scale, to be presented in the next section, the flux of Cas A was 6492 Jy, within 1% .) The secondary standards on Wyllie's scale were thus closely consistent with the scale based on the Cas A spectrum.

The overall situation with the reliability of the Cas A spectrum appeared significantly improved by the BH

spectrum. However, it remained difficult to connect the different surveys of ever-weaker sources to it, and alternative schemes of calibration were proposed. Beverley Wills [56] (in some papers by the Gorkii group, she was assumed to be masculine) published in 1973 a slightly different approach to the available absolute measurements of Cas A. In particular, she used only the early artificial-moon measurements of the early 1960s, which later were subjected by the authors to some corrections based on their work around 1970. BH used predominantly those later measurements. The spectrum of Cas A is slightly flatter in Wills' analysis. As in the works by Kellermann and colleagues, mentioned above, she selected a group of sources of intermediate strength to form the basis for a general flux-density scale.

In the years 1972-73, there were efforts to reach a general agreement on a *standard spectrum* of Cas A, and on a set of secondary standards for general use in the flux-density calibration of weak sources. The goal was to achieve a formal decision by URSI (General Assembly, Warsaw, 1972) or the International Astronomical Union (IAU, General Assembly, Sydney, 1973) to harmonize the flux-density scale. This was particularly important for the extensive source catalogues obtained with the new, powerful, large telescopes and synthesis arrays. There was some discussion at the URSI Assembly in 1972, but it did not lead to the adoption of an "officially accepted" standard Cas A spectrum or a set of secondary standards.

4.3 Extension to Weaker Sources

The interest in a further improvement of the situation with Cas A arose with this author after the publication by Dent et al. [40] of the secular decrease at 7.8 GHz being only $0.70\% \pm 0.1\%$ per year, determined over an eleven-year period. Together with data at 3.06 GHz and 9.4 GHz from Stankevich et al. [42], there appeared to be evidence of a frequency dependence of the decrease, and a fit to the available data was shown above (Equation (12)). Obviously, the data used by BH needed to be corrected for this effect, however small it might be. In addition, new accurate absolute data had become available at low frequencies between 10 MHz and 25 MHz, which could be used to clarify the downwards trend of flux density suggested by the accurate data point from Parker [18] at 38 MHz. In their latest publications, the Gorkii group had also indicated that their older measurements were in need of some correction, although the actual values of the corrections were not given (at least, not in the translated material that was available).

The author thus started to work on a revision of the BH spectrum of Cas A in the course of 1974. It was not clear how useful this would be for the actual practice of defining a flux-density scale for the large amount of data being produced by the surveys with the newest telescopes, such as the Effelsberg 100-m telescope, and the Synthesis Telescopes at Westerbork and Cambridge. It seemed that the BH paper did not have all that much of an impact on the

Source	Frequency Interval	Spectral Parameters		
		a	b	c
Cas A (1965.0)	22 MHz – 300 MHz	5.625 ± 0.021	-0.634 ± 0.015	-0.023 ± 0.001
	300 MHz – 31 GHz	5.880 ± 0.025	-0.792 ± 0.007	–
Cyg A	20 MHz – 2 GHz	4.695 ± 0.018	$+0.085 \pm 0.003$	-0.178 ± 0.001
	2 GHz – 31 GHz	7.161 ± 0.053	-1.244 ± 0.014	–
Tau A	1 GHz – 35 GHz	3.915 ± 0.031	-0.299 ± 0.009	–
Vir A	400 MHz – 25 GHz	5.023 ± 0.034	-0.856 ± 0.010	–

Table 1. The spectral parameters of the primary calibrators.

calibration habits of most observers. Clearly, one needed to build a bridge to a set of sources of intermediate intensity to act as *secondary calibrators*. These sources would preferably have the following characteristics:

1. Be sufficiently strong to serve as calibrator, but sufficiently weak to avoid linearity problems for the calibration of the very weak sources in the newest surveys;
2. Have a simple power-law spectrum over a substantial part of the radio spectrum;
3. Be constant in intensity over time and have a known, preferably zero, degree of polarization;
4. Be “point-like” for the largest interferometer baselines to avoid the need for size corrections;
5. Preferably have an accurately known position so as to be also useful for antenna pointing and baseline determination of interferometers.

Such a program was initiated at the Max-Planck-Institut für Radioastronomie (MPIfR) in Bonn, where Reinhard Genzel did the bulk of the work, guided by Ivan Pauliny-Toth and Arno Witzel. After joining the MPIfR in 1975, the author became involved in this project, which eventually led to the *calibration paper* by Baars, Genzel, Pauliny-Toth, and Witzel (BGPW), published in *Astronomy and Astrophysics* in 1977 [43].

4.3.1 The Absolute Spectrum of Cassiopeia A

In the BGPW paper, the spectrum of Cas A, along with the spectra of Cyg A and Tau A, were brought up-to-date by including new accurate measurements since 1972, replacing the old artificial-moon data by newer data, and considering the frequency dependence of the secular decrease in Cas A. An important result of the analysis was the confirmation of a downwards bending of the spectrum at frequencies below about 300 MHz. The best fit for the entire spectrum was obtained by a second-degree function between 20 MHz and 300 MHz, and a straight power-law

spectrum from 300 MHz to 30 GHz. The spectral data, including those for Cyg A, Tau A, and Vir A are given in Table 1. The parameters a , b , and c are to be used in the equation for the flux density, S :

$$\log S = a + b \log \nu + c \log^2 \nu , \quad (14)$$

with S in Jy and ν in MHz.

The spectra of these four sources, together with the data points from 200 MHz upward, are shown in Figure 9.

The authors of BGPW restricted the use of artificial-moon measurements to the period after 1967, because earlier artificial-moon measurements needed corrections, which were not described. Moreover, they also limited the number of data points to roughly the same as the number of horn data points, evenly distributed over the frequency range between 500 MHz and 9800 MHz. Using only the horn data points, the spectrum was slightly flatter ($b = -0.782$), while that of only artificial-moon data was a bit steeper ($b = -0.807$): they intersected near 2.5 GHz.

4.3.2 The Secondary Calibration Sources

The second part of the BGPW paper contained accurate spectra of about a dozen *secondary standard sources*. These were obtained from accurate ratios with respect to the primary standard sources. At the higher frequencies (> 5 GHz), Vir A, being of intermediate strength, served in this process as a convenient secondary calibrator. Flux-density ratios were collected, both from the literature and by additional observations, at eleven frequencies over the range from 0.4 GHz to 15 GHz. The derived spectra had an absolute accuracy of better than 5%. Three of the sources (3C48, 3C147, and 3C286) were also suitable for the calibration of interferometers of moderately high resolution, and have been universally used for this purpose. The BGPW paper also presented an updated table of correction factors to earlier flux-density scales. Finally, it included a table of the flux density of 14 secondary calibrators at eight widely used *standard* observing frequencies.

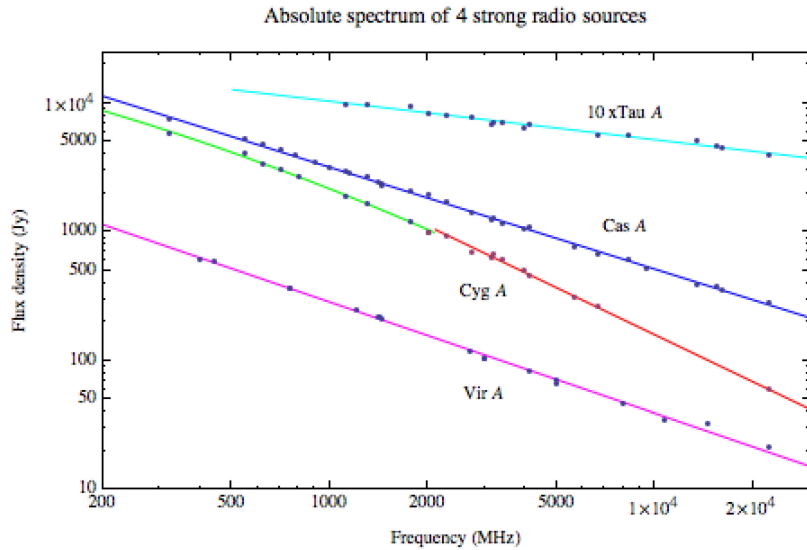


Figure 9. The absolute spectrum of Cas A from 300 MHz to 25 GHz, based on 30 absolute measurements with horn or artificial moon, as well as the absolute spectra of Cyg A and Tau A, and the semi-absolute spectrum of Vir A.

It was probably mainly through the accurate data on already widely used secondary calibrators that the paper was generally accepted as the basis for the flux-density calibration of radio-source observations. It has been cited more than 1700 times since its publication. Obviously, most observers were content. However, with the growing amount of data, made with sensitive and high-resolution telescopes, it became clear that several of the secondary standard sources showed significant variability over time. The extrapolation to frequencies above 20 GHz was also not perfect. Ott et al. [57] improved the consistency of the set by new observations over a wide frequency range up to 43 GHz. They found 3C286 and 3C295 to be very constant in flux density, and used these as a link between the BGPW scale and the other secondary calibrators.

4.4 Extension to Higher Frequencies and a New Scale

Despite some adjustments and corrections to the set of most-suitable secondary standards, the basic BGPW flux-density scale remained generally used over the last 35 years. The scale essentially became detached from the evolution of the Cas A spectrum over time. One could say that Cas A had fulfilled its purpose, and could further be studied on its own merit by making high-angular-resolution maps, and following in detail its decrease in flux density. The author is aware of one high-accuracy absolute measurement at 32 GHz by Mason et al. [58]. The measured flux density was $194.5 \text{ Jy} \pm 2.5 \text{ Jy}$ at epoch 1998.4. The BGPW spectrum

predicts a flux density of 205 Jy at epoch 1965, suggesting a decrease of only 10 Jy over more than 30 years, or an annual decrease of about 0.15%. This is considerably smaller than expected from Equation (13), but is perhaps consistent with the later values given by the Gorkii group (see Figure 8). It can also be an indication of a deviation of the spectrum from the straight power law valid to 25 GHz. There are indeed indications from the Wilkinson Microwave Anisotropy Probe (WMAP) data (23 GHz to 94 GHz) that the spectrum flattens over that frequency range (Weiland et al. [59]).

The emergence of large and powerful mm-wavelength telescopes in the 1980s increased the need to extend the flux-density scale to frequencies well in excess of 100 GHz. This aspect will be discussed in the next section. Although the powerful synthesis arrays and VLBI networks were primarily interested in accurate positions of point sources for the position calibration of new sources, their sensitivity pushed detection limits into the millijansky region, which put additional requirements on the accuracy and reliability of the existing secondary calibrators.

At the NRAO Very Large Array (VLA) in New Mexico, Rick Perley and Bryan Butler used the frequency flexibility and high sensitivity of the VLA over almost 30 years (1983–2012) to monitor the set of secondary calibrators with respect to each other and with respect to the planet Mars. This led to an accurate flux-density scale from 1 GHz to 50 GHz (Perley and Butler [4]), which we will now summarize.

Source	<i>a</i>	<i>b</i>	<i>c</i>	<i>d</i>
3C123	1.8077 ± 0.0036	-0.8018 ± 0.0081	-0.1157 ± 0.0047	0
3C196	1.2969 ± 0.0040	-0.8690 ± 0.0114	-0.1788 ± 0.0150	0.0305 ± 0.0063
3C286	1.2515 ± 0.0048	-0.4605 ± 0.0163	-0.1715 ± 0.0208	0.0336 ± 0.0082
3C295	1.4866 ± 0.0036	-0.7871 ± 0.0110	-0.3440 ± 0.0160	0.0749 ± 0.0070

Table 2. The coefficients of the fitted spectra for the four steady sources.

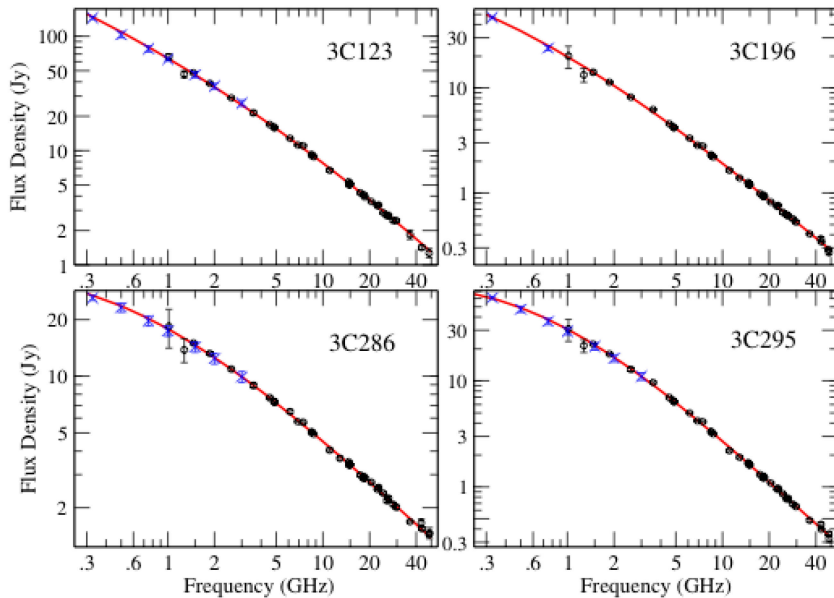


Figure 10. Spectra of the four non-variable standard calibrator sources. The black dots are measurements based on the Mars model. The red line is the best fit, according to Table 2. Data based on the BGPW or Scaife and Heald scale are indicated by a cross. Note the excellent fit of these data to the spectra (after Perley and Butler [4]).

The program started in 1983, with the complete secondary calibrator list from BGPW. The seven most compact of these were carried through the entire program. Over time, other objects were added, including several planets. Observations were carried out in all frequency bands of the VLA, nine in total, covering the frequency range from 300 MHz up to 50 GHz. Data were collected during nineteen sessions of typically two days, up to early 2012. The planet Mars was used as a high-frequency standard, and the absolute calibration of Mars by WMAP made it possible to put the flux-density scale over the entire cm-wavelength range on an absolute basis. This also enabled a direct comparison with the BGPW scale. The measurements of the source intensity ratios showed that four sources (3C123, 3C196, 3C286, and 3C295) were constant in output to better than 1% over the duration of the program. These were put on the Mars scale to serve as *semi-primary standards*, with an estimated error of 1% in the range 4 GHz to 15 GHz, increasing to 2.5% at 1.5 GHz, 2% at 22 GHz, and 3% at 43 GHz. This small error, and the extension of the frequency range, constituted an improvement over the BGPW scale. However, a comparison with the BGPW scale showed a difference of less than 2% over the BGPW frequency range from 300 MHz upwards. It thus appears that observers who used BGPW over the last 35 years do not need to recalibrate their data.

The parameters for these four standard sources are shown in Figure 10 and in Table 2. The coefficients in the table pertain to a cubic-polynomial fit to the measured data of the form

$$\log S = a + b \log \nu + c \log^2 \nu + d \log^3 \nu, \quad (15)$$

where the flux density, S , is in Jy, and the frequency, ν , is in GHz.

4.5 Low Frequency (<300 MHz) Calibration

With the emergence of large interferometric arrays, operating with a wide bandwidth over the frequency region from about 20 MHz to 400 MHz, exemplified by LOFAR [60] and the future Square Kilometre Array (SKA) [61], the flux-density scale for that range has received closer scrutiny in recent years.

The reliability of the absolute Cas A spectrum below 150 MHz has been put in doubt as a result of the detection of short-term variations in its flux density, notably at frequencies below 80 MHz [41]. This also leads to uncertainty in the rate of secular decrease at the low frequencies and, by implication, the validity of the assumed functional form of the secular decrease over the broad frequency range up to tens of gigahertz.

To avoid this complication, Roger, Bridle, and Costain [62] constructed a flux-density scale for low frequencies based on Cyg A. This early scale was 5% below the later BGPW scale at 22 MHz. The PAPER collaboration (Parsons et al. [63] based their calibration at 150 MHz on the BGPW spectrum of Cyg A, as did Cohen et al. [64] for the VLA survey at 74 MHz. The BGPW spectrum of Cyg A in the low-frequency region was based on direct absolute measurements, mostly with interferometer systems, which minimized the influence of the considerable background brightness structure in that area of sky. Cyg A appears indeed to be the best choice of primary standard between 20 MHz and 500 MHz.

Scaife and Heald [65] addressed the need for an accurate broadband flux-density scale at low frequencies, and presented model spectra of six bright 3C radio sources in the frequency range of 30 MHz to 300 MHz. They also avoided the problem of Cas variability and put the spectra

on the scale of Roger [62], which was based on Cyg A. The deviation of their scale with respect to the BGPW scale was less than 10%. This difference might have been made smaller by the use of the BGPW absolute spectrum of Cyg A as the basis for the scale. In any case, the model spectra of the proposed six “secondary” calibration sources (3C196, 3C286, and 3C295 overlap with the Perley and Butler group) formed a good initial basis for flux-density calibration from 30 MHz to 300 MHz with LOFAR and other large low-frequency telescopes.

5. The Millimeter Wavelength Region

5.1 Early Efforts, Planets

Radio astronomers normally designate the frequency range from 30 GHz to 300 GHz as the millimeter-wavelength region. Above 300 GHz extends the sub-millimeter region. (The terahertz range starts at 1 THz, or 0.3 mm wavelength, although in branches outside astronomy, the term terahertz appears to be applied from about 300 GHz upwards.) The first small reflector antennas of about 5 m diameter, specifically designed to work up to a frequency of at least 100 GHz (a wavelength of 3 mm) appeared in the mid-1960s at the University of Texas and the Aerospace Corporation. Receiver technology for this frequency range

was in its infancy. Nevertheless, the NRAO undertook to build a mm-wavelength telescope of 10 m diameter, capable of operation at 1 mm wavelength. This *36-ft telescope* was situated at 2000 m altitude on Kitt Peak, Arizona, to exploit the superior atmospheric conditions of this dry and cloudless region. After the detection of the spectral line of carbon monoxide at 115 GHz with this instrument by Wilson, Jefferts, and Penzias [66], millimeter astronomy became a “hot” subject, and in the following decades a number of large and accurate mm-wavelength telescopes came into operation.

The exploration of the mm-wavelength range necessitated the extension of the flux-density scale to higher frequencies. A straightforward extension of the spectra of existing calibration sources posed a serious difficulty. All secondary standard sources, exhibiting a negative spectral index, were too weak to fulfill their purpose, while sources like Cas A and Tau A were *extended* sources with respect to the narrow beamwidth of the mm-wavelength telescopes, and showed considerable structure in their brightness distribution.

The planets provided an attractive alternative for standard sources. Their approximate blackbody spectrum assured increasing flux density at higher frequencies, and their angular size appeared suitable for the 10-m class of mm-wavelength telescope. However, there are also complications in the use of the planets, caused by variations

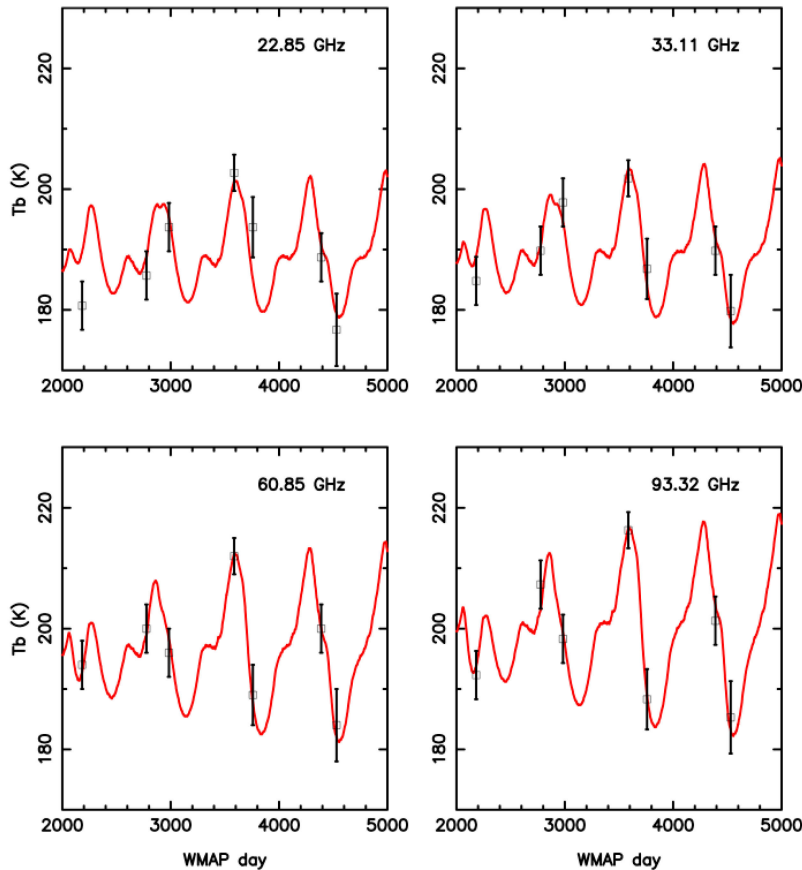


Figure 11. The brightness temperature of Mars at four frequencies, as predicted from the Rudy model over a seven-year period, shown as a continuous line, slightly adjusted to the WMAP observations shown as the black data points. The regular oscillations were due to a combination of the orbital motions of the Earth and Mars, the inclination of Mars, and the Martian seasonal variations (after Perley and Butler [4]).

in the distance (Mars), frequency dependence caused by planet's atmosphere (Venus, Jupiter), or orientation (Saturn's rings). It was thus necessary to determine their mm-wavelength spectrum by direct measurement with a calibrated antenna system. Bobby Ulich and colleagues took this up with the 4.9 m telescope in Texas, which in 1967 had been relocated to the 2000 m high site of Mt. Locke in Western Texas (Ulich et al. [67]). They calibrated the antenna with the aid of a transmitter at a distance close to the far-field limit at 3.5 mm and 2.1 mm, and observed several planets with quoted absolute accuracies of better than 10%. After moving to NRAO, Ulich used the new 36-ft telescope to improve the situation, and in 1981, proposed a set of *millimeter-wavelength calibration sources* for the range from 30 GHz to 150 GHz, with accuracies between 5% and 10% [68]. This was about as good as one could do at the time.

With the growing body of planetary observations, it became clear that none of them was without some difficulties. Observations in the 1980s with the larger millimeter and sub-millimeter telescopes and the VLA showed that Mars was the most suitable candidate to serve as primary calibrator at mm-wavelengths. First of all, it is the only planet whose observed brightness temperature is as expected from solar heating. In addition, important data on the Martian surface characteristics were provided by space probes (Viking, Mariner, Mars Global Surveyor), which allowed a detailed thermal model of the Martian surface to be constructed (Wright [69], Rudy et al. [70]). These models showed that the brightness temperature of Mars varies considerably with time, due to its position with respect to the sun and its distance and inclination with respect to the Earth, but these are readily calculable.

The space-borne observatories WMAP, Herschel, and Planck were all designed with the aim to achieve very high absolute intensity calibration, of the order of 1%. Notably, the seven-year run of WMAP provided essential data for the comparison with the planetary thermal models. This is illustrated in Figure 11, which shows the model predictions from Rudy as a function of time (in "WMAP days"), and WMAP data points at four frequencies between 22 GHz and 93 GHz. The best fit was obtained by adjusting the Rudy model by 2.6%, 3.0%, 1.5%, 1.3%, and 1.3% at 22 GHz, 33 GHz, 41 GHz, 61 GHz, and 93 GHz, respectively. One could see that the fit is excellent, but also that using Mars as a routine calibration source involves an elaborate time-dependent procedure.

Using these excellent data, Perley and Butler [4] based their flux-density scale on Mars. They achieved a total error of 2.5% at 1.5 GHz, 1% at 4 GHz to 15 GHz, 2% at 22 GHz, and 3% at 43 GHz. The WMAP accuracy was about 2% at 22 GHz, improving to 0.5% at 93 GHz. Data from the Herschel and Planck satellite telescopes extended the absolute calibration of Mars to about 1 THz with an accuracy of a few percent.

Similarly to the situation in the cm-wavelength band, also at mm-wavelengths, the somewhat cumbersome primary calibrator has been used to establish a set of *secondary calibrators* by accurate ratio determinations. Dominant here are the planets Uranus and Neptune. In connection with the sub-millimeter space missions of Herschel and Planck, detailed models of their radiation spectrum were made, which were well confirmed by observations with these telescopes. The measured brightness-temperature spectra of these bodies are not exactly "blackbody" because the wavelength dependence of the penetration depth at which the brightness is sampled. Also, Uranus exhibited a slow variation in brightness, due to the change in the sub-Earth-point latitude (Kramer et al. [71]). The accuracy of the absolute scale based on these objects was quoted as 4%. A few compact Galactic thermal sources (DR21, NGC7027, MWC349, W3(OH)) were used as secondary calibrators, but they required regular crosschecks with the primary standards because of time variability.

The accurate absolute calibration at millimeter and sub-millimeter wavelengths owed much to the space observatories mentioned above. From their position at the L2-Lagrangian point in the solar system, they avoided several of the external influences, which make highly accurate calibration from the Earth difficult. Thanks to these telescopes, the accuracy of flux-density calibration in the mm-regime is now comparable to that in the cm-region, at a level of a few percent.

5.2 ALMA Flux-Density Calibration

Around the turn of the century, three proposals for a large interferometric array, to be located at a very good site (high and dry), were joined into one global collaborative project by the initiatives from North America (NRAO in the USA and Canada), Europe (coordinated by ESO, with the participation of, at the time, ten countries), and East Asia (Japan and Taiwan) [72]. The result was the Atacama Large Millimeter/submillimeter Array (ALMA), hosted by Chile on the 5000 m high Chajnantor plateau in the northern Atacama Desert. It is an interferometric synthesis telescope consisting of 50 reflector antennas of 12 m diameter, configurable with baselines varying from 20 m up to 15 km. The antennas are equipped with low-noise cryogenic receivers, covering the entire frequency range from 30 GHz to 950 GHz, distributed over 10 bands. A small "compact array" of four 12-m antennas and a dozen 7-m dishes provide data in the spacing area below 100 m. At the time of writing (early 2014), all 66 antennas have been accepted, and most are equipped with receivers covering up to seven receiver bands. Currently, observations are being made with 45 antennas. It is expected that by the end of 2014, the full array will become available.

In the original specification, made in 2000, a goal of 1% in flux-density calibration was mentioned. The electronic system has been designed to approach this goal

by extensive calibration devices and carefully executed focal-plane optical arrangements. A major problem for an interferometric array operating at mm-wavelengths is the influence of the troposphere. Even at the superb ALMA site, the remaining water vapor along the line of sight fluctuates both in time and in the space across the array baselines, causing phase fluctuations in the interference fringes that are indistinguishable from any phase variation due to the astronomical object. These fluctuations are partially removed by alternatively observing the target source and a nearby known point source as a phase reference. The total system phase calibration is achieved with the aid of a grid of about 30 point sources evenly distributed over the sky.

By including solar-system objects in the grid, the flux-density scale is established, and the phase calibrators also serve as secondary flux-density calibrators. The scale is thus tied to the objects Mars, Uranus, Neptune, some of the planetary moons, and the asteroids Pallas, Vesta, and Ceres. The primary calibration object is Uranus, using the emission model ESA4 for its brightness. The comparison with the calibration of the Planck and Herschel space telescopes via the Mars emission model fits within 5%.

Currently, a realistic goal for absolute intensity calibration is better than 5% over the entire frequency band (80 GHz to 950 GHz). Improvements will be achieved through regular accurate relative measurements of the different objects, and detailed comparison with the theoretical emission models. A relative accuracy of 3% over the entire frequency range appears achievable. The original goal of 1% for the absolute flux-density scale may be unrealistic, but with much effort, 3% might be reached.

6. Conclusion

Obtaining reliable, accurate, quantitative results has always been, and remains to be, a major problem for the observational astronomer. A notable example is the decades-long effort to reach agreement on the value of the Hubble constant [73]. Radio astronomers have been concerned about the calibration of the intensity of radio sources from early on, not the least because radio data are being collected over several decades of wavelength, compared to the one octave in optical astronomy. Establishing a reliable spectrum over a large frequency range is essential for the interpretation of the radiation mechanism.

Perhaps also caused by their background as experimental physicists, the pioneers of absolute flux-density measurements made an essential contribution to the quantitative level of radio astronomy. Their work was, in John Findlay's words, "utterly boring but extremely important." The choice of Cas A, being the most-intense object, as original primary standard source was natural. However, the time variability of its strength made it less suitable for this purpose, albeit providing interesting data about its astrophysics. Nevertheless, a flux-density

scale based on Cas A was established over a significant frequency range of roughly 30 MHz to 30 GHz, which was used for more than 30 years. The strong interest in higher frequencies, up to 1 THz, has shifted the primary-standard role to the planets, in particular Mars. The advances in detailed planetary-emission models, confirmed or slightly adjusted by the extremely accurate calibration of the space-borne telescopes WMAP, Herschel, and Planck, provide an absolute flux-density scale based primarily on Mars with an accuracy of a few percent from 30 GHz up to several hundreds of GHz. With the good overlap of this scale with the Cas A-based scale at lower frequencies, observations over the entire radio-wavelength regime enable the determination of intrinsic source intensities with an accuracy of a few percent.

Returning to the VLA observer on the way along US Route 60 to the VLA, the observer will still be wondering how far away is the oncoming vehicle, but the observer need not be too worried about the true intensity of the objects being observed.

7. Acknowledgement

At NRAO in 1964, Peter Mezger initiated my interest in the subject. In writing this review, I became again aware of the importance of the tedious work by the colleagues who measured absolute flux densities with special antennas. Regular discussions over the years with Rick Perley kept my interest in this field active. I thank him, Richard Hills, Ruediger Kneissl, Carsten Kramer, and Ken Kellermann, as well as the referees, for helpful comments and suggestions.

8. References

1. J.D. Kraus, *Radio Astronomy*, New York, McGraw-Hill, 1966.
2. J. W. Findlay, "Absolute Intensity Calibration in Radio Astronomy," *Annual Reviews of Astronomy and Astrophysics*, **4**, 1966, pp. 77-94.
3. V. P. Ivanov and K. S. Stankevich, "Absolute Flux Scale for Radioastronomy," *Radiophysics and Quantum Electronics*, **29**, 1986, pp. 1-22.
4. R. A. Perley and B. J. Butler, "An Accurate Flux Density Scale from 1 to 50 GHz," *Astrophysical Journal Supplement*, **204**, February, 2013, p. 19-38.
5. K. G. Jansky, "Electrical Disturbances apparently of Extraterrestrial Origin," *Proceedings IRE*, **21**, 1933, pp. 1387-1398.
6. G. Reber, "Cosmic Static," *Astrophysical Journal*, **91**, 1940, pp. 621-624.
- 7a. H. I. Ewen and E. M. Purcell, "Radiation from Galactic Hydrogen at 1420 Mc/s," *Nature*, **168**, p. 356.
- 7b. C. A. Muller and J. H. Oort, "The Interstellar Hydrogen Line at 1420 Mc/s and an Estimate of Galactic Rotation," *Nature*, **168**, pp. 357-358.

8. S. Silver, *Microwave Antenna Theory and Design*, New York, McGraw-Hill, 1949.
9. Ch. I. Seeger, "A Tentative Measure of the Flux Density of Cassiopeia A at 400 Mc/s," *Bulletin Astronomical Institutes of the Netherlands*, **13**, 472, 1956, pp. 100-104.
10. D. V. Wyllie, "An Absolute Flux Density Scale at 406 MHz," *Monthly Notices Royal Astronomical Society*, **142**, 1969, pp. 229-240.
11. S. A. Schelkunoff and H. T. Friis, *Antennas: Theory and Practice*, John Wiley & Sons, 1952.
12. S. A. Schelkunoff, *Electromagnetic Waves*, New York, Van Nostrand, 1943.
13. E. V. Jull and E. P. Deloli, "An Accurate Absolute Gain Calibration of an Antenna for Radio Astronomy," *IEEE Transactions Antennas and Propagation*, **AP-12**, 1964, pp. 439-447.
14. V. S. Troitskii and N. M. Tseytlin, "The Application of the Radio-Astronomical Method for Calibrating small Antenna Systems at Centimeter Wavelengths," *Radiofizika (Russ)*, **5**, 4, 1962, pp. 623-628.
15. J. W. M. Baars, "The Paraboloidal Reflector Antenna in Radio Astronomy and Communication," New York, Springer, 2007.
16. J. W. Findlay, H. Hvatum, and W. B. Waltman, "An Absolute Flux-Density Measurement of Cassiopeia A at 1440 MHz," *Astrophysical Journal*, **141**, 1965, pp. 873-884.
17. E. A. Parker, "Precise Measurements of the Flux Densities of the Radio Sources Cas A and Cyg A at Metre Wavelengths," *Monthly Notices Royal Astronomical Society*, **138**, 1968, 407-422.
18. R. S. Roger, C. H. Costain, and J. D. Lacey, "Spectral Flux Densities of Radio Sources at 22.25 MHz," *Astronomical Journal*, **74**, 1969, pp. 366-372.
19. M. R. Viner, "26.3-MHz Radio Source Survey. I. The Absolute Flux Scale," *Astronomical Journal*, **80**, 1975, p. 83
20. A. H. Bridle, "Flux Densities of Cassiopeia A and Cygnus A at 10.05 MHz," *Observatory*, **87**, 1967, pp. 60-63.
21. S. Y. Braude, O. M. Lebedeva, A. V. Megn, B. P. Ryabov, and I. N. Zhouck, "The Spectra of Discrete Radio Sources at Decametric Wavelengths," *Monthly Notices Royal Astronomical Society*, **143**, 1969, pp. 289-300.
22. Ch. L. Seeger, "The Radio Frequency Spectrum of Cassiopeia A: A Symposium Summary," *IAU Symposium No. 5: Radio Astronomy*, Cambridge, Cambridge University Press, 1956, pp. 156-158.
23. N. W. Broten and W. J. Medd, "Absolute Flux Measurements of Cassiopeia A, Taurus A, Cygnus A at 3200 Mc/s," *Astrophysical Journal*, **132**, 1960, pp. 279-285.
24. D. A. McCrea and E. R. Seaquist, "Flux of Cas A and Cyg A at 320 Mc/s," *Astronomical Journal*, **68**, 1963, p. 77.
25. J. W. Findlay, "The Flux Density of Cassiopeia A at 1440 MHz and Its rate of Decrease," *Astrophysical Journal*, **174**, 1972, pp. 527-528.
26. W. J. Medd, "Absolute Flux Density Measurements at Centimeter Wavelengths," *Astrophysical Journal*, **171**, 1972, pp. 41-50.
27. R. J. Allen and A. H. Barrett, "Absolute Measurements of the Radio Flux from Cassiopeia A and Taurus A at 3.64 and 1.94 cm," *Astrophysical Journal*, **149**, 1967, pp. 1-13.
28. P. J. Encrenaz, A. A. Penzias, R. W. Wilson, "Flux of Cassiopeia A at 1415 MHz," *Astrophysical Journal*, **160**, 1970, pp. 1185-1186.
29. A. A. Penzias and R. W. Wilson, "Measurement of the Flux Density of CAS A at 4080 Mc/s," *Astrophysical Journal*, **142**, 1965, pp. 1149-1155.
30. R. W. Wilson and A. A. Penzias, "The Flux Density of Six Radio Sources at 4.08 GHz," *Astrophysical Journal*, **146**, 1966, p. 286.
31. G. T. Wrixon, J. R. Gott, and A. A. Penzias, "Absolute Measurements of the Flux of Cassiopeia A and Taurus A at 1.87 Centimeters," *Astrophysical Journal*, **165**, 1971, pp. 23-28.
32. G. T. Wrixon, J. R. Gott, and A. A. Penzias, "Absolute Measurements of the Flux of Cassiopeia A and Taurus A at 1.87 Centimeters," *Astrophysical Journal*, **174**, 1972, pp. 399-400 (correction to 1971 paper).
33. L. N. Bondar, M. R. Zelinskaya, et al., "Absolute Measurements of the Intensity of the Radio Emission of the Discrete Source Cassiopeia-A and Cygnus-A at Wavelengths of 30-60 cm," *Radiofizika*, **12**, 6, 1969, pp. 807-812.
34. D. A. Dmitrenko, N. M. Tseytlin, L. V. Vinogradova, K. F. Gitterman, "Absolute Measurements of the Intensity of Radio Emission from Cassiopeia-A, Cygnus-A, Taurus-A in the Range 3-15 cm," *Radiofizika*, **13**, 6, 1970, pp. 823-829.
35. L. V. Vinogradova, D. A. Dmitrenko, and N. M. Tseytlin, "Absolute Measurements of the Intensity of Radio Emission from Cassiopeia-A, Cygnus-A, Taurus-A in the range 15-30 cm," *Radiofizika*, **14**, 1, 1971, pp. 157-159.
36. I. S. Shklovskii, "Secular Variation of the Flux and Intensity of Radio Emission from Discrete Sources," *Soviet Astronomy*, **4**, 1960, pp. 243-249.
37. J. A. Högbom and J. R. Shakeshaft, "Secular Variation of the Flux Density of the Radio Source Cassiopeia A," *Nature*, **189**, 1961, pp. 561-562.
38. J. W. M. Baars and A. P. Hartsuijker, "The Decrease of Flux Density of Cassiopeia A and the Absolute Spectra of Cassiopeia A, Cygnus A and Taurus A," *Astronomy & Astrophysics*, **17**, 1972, pp. 172-181.
39. P. F. Scott, J. R. Shakeshaft, M. A. Smith, "Decrease of Flux Density of the Radio Source Cassiopeia A at 81.5 MHz," *Nature*, **223**, 1969, pp. 1139-1140.
40. W. A. Dent, H. D. Aller, E. T. Olsen, "The Evolution of the Radio Spectrum of Cassiopeia A," *Astrophysical Journal*, **188**, 1974, L11-L13.
41. P. L. Read, "Measurement of the Flux Density of Cas A and Confirmation of an Anomaly at 38 MHz," *Monthly Notices Royal Astronomical Society*, **178**, 1977, pp. 259-264; also **181**, 1977, p. 63.
42. K. S. Stankevich, V. P. Ivanov, S. A. Peljuschenko, V. A. Torchov, A. N. and Ibannikova, "Radio Radiation from the Supernova Remnant Cassiopeia A," *Radiofizika*, **16**, 1973, pp. 786-798.

43. J. W. M. Baars, R. Genzel, I. I. K. Pauliny-Toth, A. Witzel, "The Absolute Spectrum of Cas A; An Accurate Flux Density Scale and a Set of Secondary Calibrators," *Astronomy & Astrophysics*, **61**, 1977, pp. 99-106.
44. K. S. Stankevich, V. P. Ivanov, and S. P. Stolyarov, "Fifty Years of Radio Observations of the Discrete Source Cassiopeia A," *Astronomy Letters*, **25**, 1999, pp. 501-507.
45. C. O'Sullivan and D. A. Green, "Constraints on the Secular Decrease in the Flux Density of Cas A at 13.5, 15.5 and 16.5 GHz," *Monthly Notices Royal Astronomical Society*, **303**, 1999, pp. 575-578.
46. Y. A. Hafez, R. D. Davies et al., "Radio Source Calibration for the VSA and Other CMB Instruments at Around 30 GHz," *Monthly Notices Royal Astronomical Society*, **388**, 2008, pp. 1775-1786.
47. E. N. Vinyaikin, "Evolution of the Radio Emission of the Crab Nebula from Long-term Observation at 927 and 151.5 MHz," *Astronomy Reports*, **51**, 2007, pp. 570-576.
48. H. D. Aller and S. P. Reynolds, "The Decrease with Time of the Radio Flux of the Crab Nebula," *Astrophysical Journal*, **293**, 1985, pp. L73-L75.
49. G. R. Whitfield, "The Spectra of Radio Stars," *Monthly Notices Royal Astronomical Society*, **117**, 1957, pp. 680-691.
50. R. G. Conway, K. I. Kellermann, and R. J. Long, "The Radio Frequency Spectra of Discrete Radio Sources," *Monthly Notices Royal Astronomical Society*, **125**, 1963, pp. 261-284.
51. K. I. Kellermann, "Measurements of the Flux Density of Discrete Radio Sources at decimeter Wavelengths," *Astronomical Journal*, **69**, 1964, pp. 205-214.
52. K. I. Kellermann, I. I. K. Pauliny-Toth, and P. J. S. Williams, "The Spectra of Radio Sources in the Revised 3C Catalogue," *Astrophysical Journal*, **157**, 1969, pp. 1-34.
53. J. W. M. Baars, P. G. Mezger, and H. Wendker, "The Spectra of the Strongest Non-Thermal Radio Sources in the Centimeter-Wavelength Range," *Astrophysical Journal*, **142**, 1965, pp. 122-134.
54. S. von Hoerner, "Design of Large Steerable Antennas," *Astronomical Journal*, **72**, 1967, pp. 35-47.
55. R. G. Conway and R. E. B. Munroe, "The Ratio of Two Flux Density Scales," *Monthly Notices Royal Astronomical Society*, **159**, 1972, pp. 21P-24P.
56. B. J. Wills, "On the Calibration of Flux Densities and the Determination of Spectra at Radio Frequencies," *Astrophysical Journal*, **180**, 1973, pp. 335-350.
57. M. Ott, A. Witzel et al., "An updated List of Radio Flux Density Calibrators," *Astronomy & Astrophysics*, **284**, 1994, pp. 331-339.
58. B. S. Mason, E. M. Leitch, S. T. Myers, J. K. Cartwright, and A. C. S. Readhead, "An Absolute Flux Density Measurement of the Supernova Remnant Cassiopeia A at 32 GHz," *Astronomical Journal*, **118**, 1999, pp. 2908-2918.
59. J. L. Weiland, N. Odegard et al., "Seven-year Wilkinson Microwave Anisotropy Probe (WMAP) Observations: Planets and Celestial Calibration Sources," *Astrophysical Journal Supplement*, **192**, February, 2011, pp. 19-40.
60. M. P. van Haarlem et al., "LOFAR: The Low-Frequency Array," *Astronomy & Astrophysics*, **556**, 2013, p. A2.
61. P. E. Dewdney, P. J. Hall, R. T. Schilizzi, and T. J. L. W. Lazio, "The Square Kilometre Array," *Proceedings of the IEEE*, **97**, 2009, pp. 1482-1496.
62. R. S. Roger, A. H. Bridle, C. H. Costain, "The Low-Frequency Spectra of Nonthermal Radio Sources," *Astronomical Journal*, **78**, 1973, pp. 1030-1057.
63. A. R. Parsons, D. C. Backer et al., "The Precision Array for Probing the Epoch of Reionization: Eight Station Results," *Astronomical Journal*, **139**, 2010, pp. 1468-1480.
64. A. S. Cohen, W. M. Lane et al., "The VLA Low-Frequency Sky Survey," *Astronomical Journal*, **134**, 2007, pp. 1245-1262.
65. A. M. M. Scaife and G. H. Heald, "A Broadband Flux Scale for Low Frequency Radio Telescopes," *Monthly Notices Royal Astronomical Society*, **423**, 2012, pp. L30-L34.
66. R. W. Wilson, K. B. Jefferts, and A. A. Penzias, "Carbon Monoxide in the Orion Nebula," *Astrophysical Journal*, **161**, 1970, pp. L43-L44.
67. B. L. Ulich, J. H. Davis, P. J. Rhodes, and J. M. Hollis, "Absolute Brightness Temperature Measurements at 3.5-m Wavelength," *IEEE Transactions Antennas and Propagation*, **AP-28**, 1980, pp. 367-377.
68. B. L. Ulich, "Millimeter-Wavelength Continuum Calibration Sources," *Astronomical Journal*, **86**, 1981, pp. 1619-1626.
69. E. L. Wright, "Recalibration of the Far-infrared Brightness Temperatures of the Planets," *Astrophysical Journal*, **210**, 1976, pp. 250-253.
70. D. J. Rudy, D. O. Muhleman, G. L. Berge, B. M. Jakosky, and P. R. Christensen, "Mars: VLA Observations of the Northern Hemisphere and the North Polar Region at Wavelengths of 2 and 6 cm," *Icarus*, **71**, 1987, pp. 159-177.
71. C. Kramer, R. Moreno, and A. Greve, "Long-Term Observations of Uranus and Neptune at 90 GHz with the IRAM 30 m Telescope," *Astronomy & Astrophysics*, **482**, 2008, pp. 359-363.
72. R. L. Brown, W. Wild, and G. Cunningham, "ALMA – The Atacama Large Millimeter Array," *Advances in Space Research*, **34**, 2004, pp. 555-559.
73. W. L. Freedman and B. F. Madore, "The Hubble Constant," *Annual Review Astronomy & Astrophysics*, **48**, 2010, pp. 673-710.